Conditional Sampling of Velocity in a Turbulent Nonpremixed Propane Jet

R. W. Schefer,* V. Hartmann,† and R. W. Dibble*
Sandia National Laboratories, Livermore, California

Simultaneous axial and radial velocities have been measured throughout a turbulent nonreacting propane jet under high Reynolds number conditions using a two-color laser velocimeter. The objective of the measurements has been to obtain a better understanding of the flow structure and mixing process in turbulent, nonpremixed, variable-density jets. Velocity measurements conditional on fluid originating from the jet and from the coflowing airstream were obtained by alternately seeding only the jet fluid and the coflowing air. In addition to information on mean and fluctuating quantities, conditionally sampled probability density distributions of axial and radial velocity and the joint probability distributions are presented. The results show that differences in the conditional velocity statistics (i.e., means and higher moments) at a location are dependent on the degree of prior mixing. In regions near the centerline where sufficient mixing has occurred, the conditionally sampled statistics agree well whereas, in the mixing region between the central jet and the outer coflowing air, insufficient mixing has occurred and significant differences are observed.

Introduction

An understanding of the process whereby chemically reactive species are mixed prior to combustion is central to the development of physically realistic models for turbulent reacting flows. Conventionally averaged point measured statistics have added greatly to our understanding of turbulent mixing and have provided data with which modeling assumptions and predictive capabilities can be tested. At the same time, they are limited by their very nature in the extent to which a true physical picture of turbulence can be developed. Since the early measurements of Corrisin and Kistler,[9] the concept of intermittency and the subsequent development of conditional sampling techniques have played an increasingly important role in identifying the important phenomena underlying turbulent mixing.

The concept of intermittency is based on the existence of clearly distinguishable turbulent and nonturbulent zones in the flowfield. Although, in a strict sense, vorticity should be used as the flow property that distinguishes between turbulent and nonturbulent fluid, it is difficult to measure experimentally. This difficulty has led to the use of velocity,[2] temperature,[5] density,[22] and concentration[17] as the discriminating function for turbulent and nonturbulent fluid zones (an excellent discussion of intermittency and conditional sampling techniques can be found in the review by Antonia[1]). Conditional sampling techniques have evolved from the need to measure the considerably different statistical properties of these zones. Recent models have been developed that incorporate intermittency and conditional statistics,[13,14,18] but comparisons with experimental measurements are presently limited and the predictive capabilities of these models have not yet been fully explored.

Two-color laser velocimetry (LV) was recently combined with a laser-Raman scattering system to obtain simultaneous measurements of velocity and scalar concentrations.[10] Measurements were obtained in a turbulent nonreacting propane jet and a reacting jet mixture of hydrogen and argon. The results of this study identified potential bias in the measured scalar value when the scalar measurement is conditioned on a valid velocity measurement. The limits of this biasing were established by adding LV seed particles only to the jet flow and only to the coflowing airstream. The results are thus biased toward fluid originating from the jet and from the coflowing air, respectively. The study concluded that seeding bias due to unequal seeding of the jet and coflowing airstream can significantly affect the scalar measurements conditioned on a velocity measurement.

The velocity data also showed significant differences in velocity statistics when the LV seed is preferentially added to the jet or the coflowing air. Although no detailed interpretation of the velocity data was presented, subsequent analysis of the data has shown that this seeding technique provides a useful marker for fluid originating from the jet and the coflowing air and that the resulting conditional velocity statistics provide considerable information on details of the mixing process between these two streams. A more detailed analysis of the conditional velocity data is presented here in terms of conditionally sampled mean and fluctuating velocities, probability density distributions of axial and radial velocity, and the joint probability distributions of axial and radial velocity.

Additional motivation for the present work comes from a recent review of experimental data in turbulent shear flows.[23] This study was undertaken with a view to developing a data base in selected nonreacting and reacting turbulent shear flows for the evaluation of current numerical modeling approaches. The review was limited to simplified geometries and flowfields that could be treated analytically by parabolic methods; turbulent variable-density jets were selected as one class of flows for review. A general conclusion of the review was that in many flows, the experimental data were insufficient for suitable comparisons with model predictions. The velocity measurements presented here are complimentary to additional scalar measurements in the same flow presented elsewhere; Rayleigh scattering was used by Schefer and Dibble[21] to measure the propane mixture fraction while, as mentioned above, Raman scattering was combined with laser velocimetry for the measurement of joint probability distributions of species concentration and velocity.[10] In each study, measure-

Received April 14, 1986; revision received Oct. 25, 1986. This paper is declared a work of the U.S. Government and is not subject to copyright protection in the United States.

*Member Technical Staff, Combustion Research Facility.

†Member Technical Staff, Combustion Research Facility, NATO Postdoctoral Research Fellow, Deutscher Akademischer Austauschdienst; currently with BMW AG, Munich, West Germany.

ments were presented along the centerline and at several transverse stations. It is hoped that the present data, combined with the additional scalar measurements cited, will provide a comprehensive data base for future comparison with and evaluation of computational models. To facilitate comparisons with modeling calculations, a complete tabulation of all experimental data taken in the present flow can be found in Ref. 20. The tabulated results include measurements of mean and fluctuating quantities, higher moments, and probability density distributions for both velocity and propane mixture fraction. Copies of the tabulated data are also available on magnetic tape and can be obtained from the authors through Sandia National Laboratories, Livermore, California.

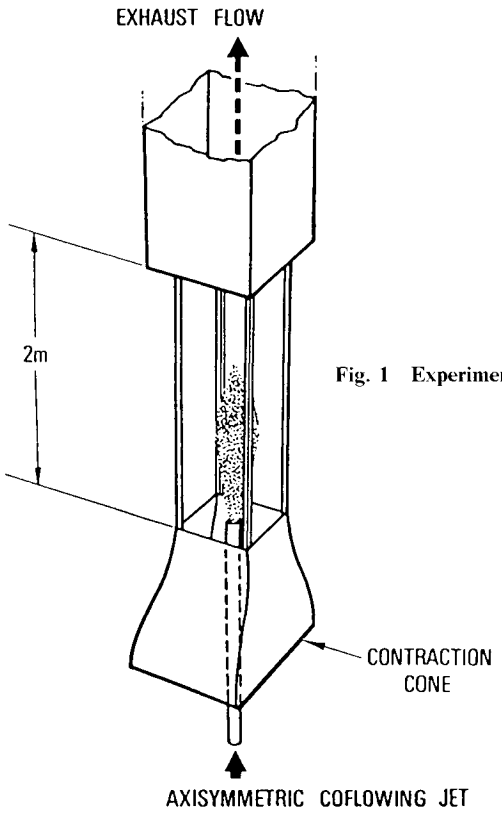

Fig. 1 Experimental test facility.

In the remainder of this paper, the experimental system will be described and the experimental results will be presented. First, axial and radial profiles of single point velocity statistics will be discussed. Next, conditionally sampled probability distributions of the axial and radial velocity will be presented and used to interpret the measured variations in axial and radial velocity with flowfield location. Finally, the joint probability density distributions of axial velocity and radial velocity will be described.

Experiment

Test Facility and Experimental Conditions

A schematic of the test section is shown in Fig. 1. The flow configuration consists of a high-velocity central jet of fuel surrounded by a coflowing airstream. Airflow rates up to 40 m/s are provided by a variable-speed centrifugal fan. Flow rates are determined from the measured pressure drop across a calibrated venturi meter located upstream of the test section. A honeycomb section located upstream of the contraction cone and a 9 : 1 area ratio across the contraction cone provide a uniform velocity across the test section entrance with a measured inlet turbulence level of 0.4%. The fuel nozzle is located at the upstream end of the test section and is aligned with the test section centerline. The fuel jet inside diameter D is 5.02 mm with the jet exit preceded by a 2-m length of straight tubing. Measurements at the test section inlet have shown that the jet inlet velocity profile corresponds to a fully developed turbulent pipe flow. Gas flows through the fuel jet are metered by mass flow controllers to an accuracy of 2%.

The test section has a 30-cm square cross section and is 200 cm long. Optical access is provided through the removable glass walls of the test section. The test section and contraction cone are mounted on a traversing mechanism driven by stepping motors to provide positioning in three directions. This allows the optical diagnostics to remain fixed and simplifies the alignment procedure.

The propane jet bulk velocity u_j in the present investigation was 53 m/s, giving a Reynolds number based on the jet exit diameter Re_j of 68,000. The coflowing air velocity u_{co} was 9.2 m/s, giving a ratio of jet to coflow air velocity of 5.76. Bulk velocity of the fuel jet was determined from the measured volumetric flow rates using a calibrated mass flow controller and the internal area of the jet nozzle. A boundary layer was also measured along the outer edge of the jet pipe with a thickness of approximately 0.3 jet diameters at the exit plane

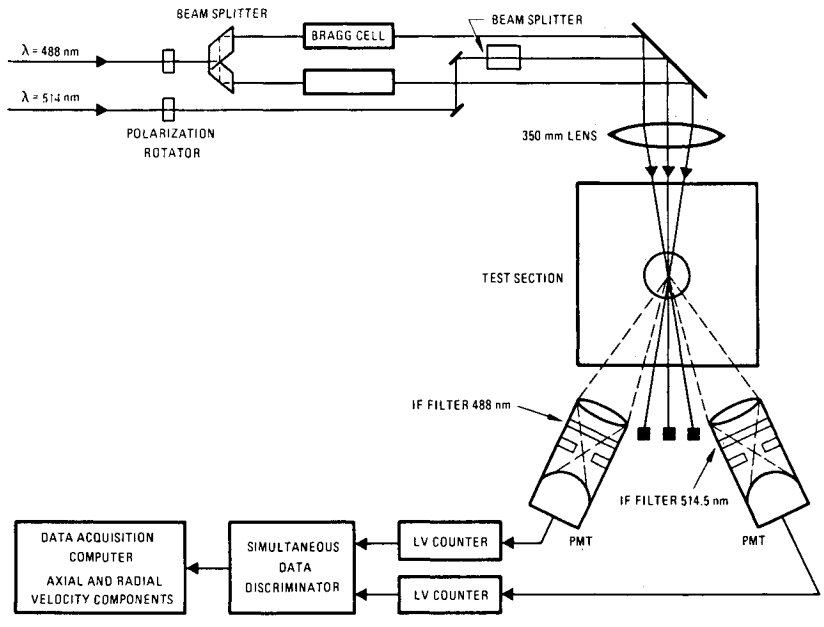

Fig. 2 Schematic of two-color LV apparatus.

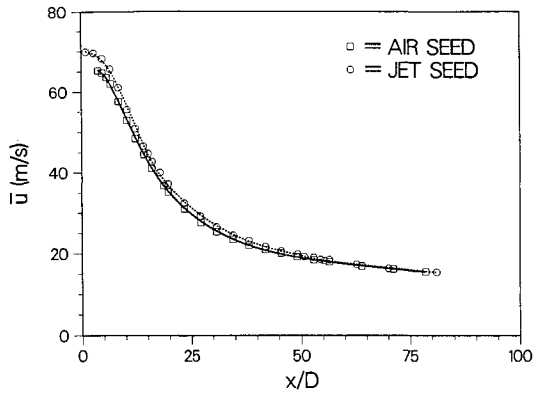

Fig. 3 Centerline variation in conditionally sampled mean velocity downstream of the jet exit. Bulk jet velocity = 53 m/s; coflowing air velocity = 9.2 m/s. Solid line indicates data collected with LDV seed added to the coflowing airstream only; dotted line indicates data collected with LDV seed added to the propane jet stream only; □, coflowing air seed only; ⊙, jet seed only.

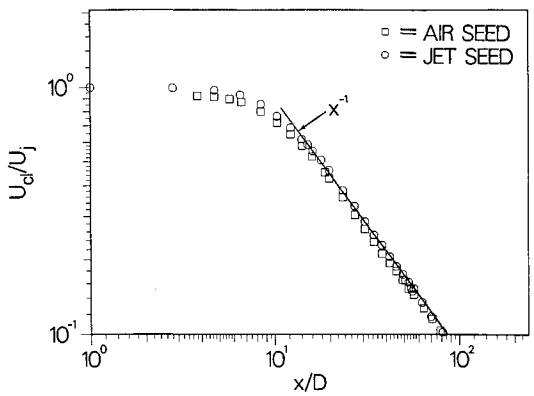

Fig. 4 Axial velocity decay along centerline shown on logarithmic scale. Bulk jet velocity = 53 m/s; coflowing air velocity = 9.2 m/s. Symbols same as Fig. 3.

of the jet. A more complete description of the inlet conditions is given in Ref. 20.

The axial pressure gradient was measured by wall pressure taps located at the test section inlet and exit. The measured value was 6 Pa/m at the flow conditions studied.

Optical System

A schematic of the laser velocimetry (LV) system is shown in Fig. 2. The laser velocimetry measurements were made with a two-color, dual-beam, real-fringe system. Axial velocities were measured using the green ($\lambda = 514.5$ nm) line from a 6-W argon-ion laser oriented with the fringe system perpendicular to the axial direction; radial velocities were measured using the blue ($\lambda = 488.0$ nm) line with the fringe pattern oriented perpendicular to the radial direction. Directional ambiguity in the radial direction was eliminated by frequency-shifting the blue beams at 10 MHz (TSI Model 9184-11 dual Bragg cell with one beam shifted at 30 MHz and the other at 40 MHz). After reflection by a turning mirror, the four beams (50-mm beam spacing) were focused to cross at the measurement volume, using a 350-mm focal length transmitting lens. The measured fringe spacing at the beam crossing was 3.74 μm for the green beams and 3.53 μm for the blue beams. The fuel stream and airstream were seeded independently with nominal 0.85-μm diameter alumina particles, using two TSI Model 3400 fluidized bed particle generators. Light scattered from the particles was collected at an angle of 15 deg to the forward direction by a 350-mm focal length lens and focused onto two pinhole-photomultiplier tube combinations. Optical filters prior to the pinholes were used to differentiate between the radial and axial velocity components. The measurement volume, as defined by the image of the pinhole (100-μm diam) on the beam crossing and the laser beam waist diameter, was 0.30 mm long × 0.20 mm in diameter. The output signal from each photomultiplier tube was filtered, processed, and validated using a counter-type processor (TSI Model 1990A). Coincidence of the radial and axial velocity measurements was verified with a multichannel interface (TSI Model 1998D-1) with a variable time window set at 10 μs to assure that the velocity measurement in each direction was from the same particle.

Data Reduction and Error Analysis

Conditional statistics were obtained for the mean and fluctuating velocities and the correlation between the axial and radial velocity $\overline{u'v'}$. At each measurement location, a minimum of 3000 velocity measurements were obtained. This was estimated to be sufficient for the first two moments of the velocity. The correlation $\overline{u'v'}$ calculated from 3000 measurements was found to agree within 1% of the value calculated from up to 10,000 measurements. In the analysis of the data, it is assumed that the seed particles follow the motion of the fluid. Since the velocity of a particle is actually measured with LV, particle velocity lag must be considered as a potential source of error. Using the estimates in Ref. 11, a 0.85-μ particle can follow the flow up to a frequency of 8 kHz with a slip velocity of 1%. Based on previous measurements in the current flow,[21] this frequency response is sufficient. An additional assumption is that the difference between the diffusivity of the particle and the fluid can be negligible. This assumption has been shown to be valid in the limit of large Reynolds number,[6] where mixing is dominated by turbulent transport. With these assumptions, the motion of a seed particle is identical to the motion of a fluid element. Thus, fluid originating from the jet can be distinguished from fluid originating from the coflowing air and, by alternately seeding only the jet streams and the coflowing airstreams, velocity statistics conditional on the jet fluid and on the coflowing air can be obtained.

The conditional measurements provided by the above seeding technique can be interpreted as a measure of the "degree of mixing" in the velocity field. That is, statistics conditional on fluid originating from the coflowing air consist of contributions from 1) unmixed air and 2) air previously entrained and subsequently mixed with jet fluid. Similarly, statistics conditional on fluid originating from the jet consist of contributions from 1) unmixed jet fluid and 2) jet fluid that has been mixed with entrained air. The measured differences in conditional quantities thus reflect the extent to which fluid originating from the two inlet streams has mixed at a small-scale level and can be attributed to the presence of larger-scale structures in the flowfield.

The principal sources of error inherent in LV (in addition to particle lag discussed above) in highly turbulent flows have been reviewed elsewhere.[11] In the present flow, the primary source of error that must be considered is bias due to the proportionality of particle flux through the measurement volume to the instantaneous velocity (velocity weighting). This may give rise to a statistical bias toward higher velocities when number-weighted averages are used to calculate stationary statistics. Razdan[19] has shown in a comparable flow that for velocity fluctuations up to 10%, the errors are negligible. As the fluctuations increase, the velocity bias toward higher velocities also increases. At the maximum fluctuation levels measured in the present flow (27%), a maximum bias error of 4% would be expected. The effect of velocity weighting bias on the mean velocity was estimated from the equations of McLaughlin and Tiederman[15] and found to be less than 2%.

Additional sources of error have also been estimated. The error due to velocity gradient broadening was estimated to be

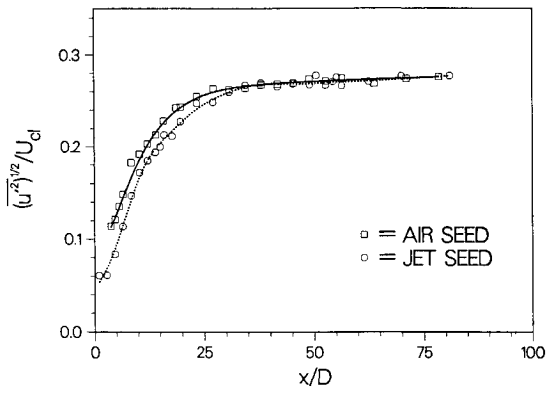

Fig. 5 Centerline variation in conditionally sampled axial velocity fluctuations downstream of jet exit. Bulk jet velocity = 53 m/s; coflowing air velocity = 9.2 m/s. Solid line indicates data collected with LV seed added to the coflowing airstream only; dotted line indicates data collected with LV seed added to the propane jet stream only; □, coflowing air seed only; ⊙, jet seed only.

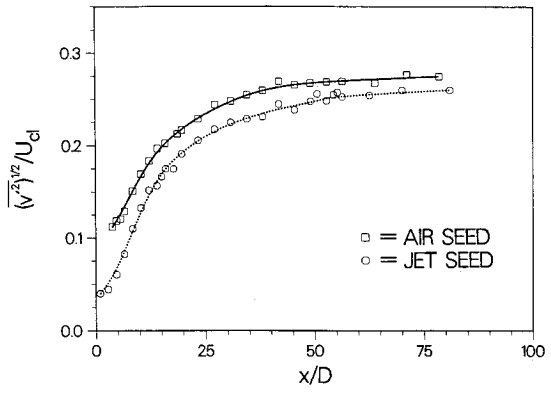

Fig. 6 Centerline variation in conditionally sampled radial velocity fluctuations downstream of the jet exit. Bulk jet velocity = 53 m/s; coflowing air velocity = 9.2 m/s. Solid line indicates data collected with LV seed added to the coflowing airstream only; dotted line indicates data collected with LV seed added to the propane jet stream only; □, coflowing air seed only; ⊙, jet seed only.

< 0.3%. Errors in time measurement with a counter processor having 0.5-ns resolution are < 0.2% at the highest burst frequencies measured, and the effects of variation in refractive index on movement of the measurement volume are negligible.

Several checks on the data were performed to assess the accuracy of the measurements. Conservation of propane (on a mass basis) was verified by integrating the velocity and propane mass fraction measurements,[21] across the flowfield. The integration was carried out at three axial locations ($x/D = 15$, 30, and 50), and the total propane mass flux was compared with the calibrated value based on the mass flowmeter reading. The total propane mass flux at the jet exit was 2.3 g/s and the mass flux calculated at each axial location agreed with this value within 5%. In addition to the conservation of propane, momentum must also be conserved across the flowfield. Integration of the total momentum at the above three axial locations was found to agree within 3% of the inlet value. The long-term repeatability of the measurements was established by repeating the measurements at selected locations after the initial data set was obtained. Data reproducibility was found to be within 2%.

Results

Axial Centerline Profiles

Mean Velocity Decay

Centerline profiles of the conditionally sampled mean axial velocity are shown in Fig. 3. In the following discussion, data conditioned on fluid originating from the jet will be denoted by the subscript "jet" (dashed line in figures), and data conditioned on fluid originating from the coflowing air by the subscript "air" (solid line in figures). Nearest the jet exit is the potential core region, which extends approximately 4 diameters downstream of the jet exit. This region is characterized by a nearly constant axial velocity of 70 m/s (based on measurements conditional on the jet fluid), which is consistent with fully developed pipe flow issuing from the jet exit at a bulk flow velocity of 53 m/s ($u_{j,\max} = 1.28u_{j,\text{bulk}}$). No measurements conditional on the coflowing air were made in this region since particles originating from the air did not penetrate to the centerline of the potential core.

Downstream from the potential core region both $\bar{u}_{\text{jet}}$ and $\bar{u}_{\text{air}}$ decrease rapidly and approach the outer coflowing air velocity of 9.2 m/s. For axial distances $x/D < 50$, $\bar{u}_{\text{jet}}$ is consistently higher than $\bar{u}_{\text{air}}$. This difference is greatest near the jet exit, where insufficient mixing has occurred between fluid originating from the jet and fluid originating from the outer coflowing air, which has been entrained by the high-velocity jet fluid, transported across the mixing zone to the centerline, and mixed with jet fluid. The differences between $\bar{u}_{\text{jet}}$ and $\bar{u}_{\text{air}}$ decrease farther downstream and, for an axial distance $x/D > 50$, the results for both cases agree within the accuracy of the measurements. This distance defines the distance required for jet fluid to become well mixed with coflowing air entrained into the jet stream. The greater differences measured near the jet exit are due to the shorter convective time scales associated with this region; near the jet exit, insufficient time is available for the velocity associated with fluid originating from regions away from the centerline to equilibrate fully with jet fluid.

The mean axial velocity decay along the centerline is replotted in Fig. 4 on logarithmic coordinates. The axial velocity is presented as centerline excess velocity U_{cl} (excess velocity is defined as the difference between the mean centerline velocity and the coflowing air velocity) and is normalized by the excess velocity at the jet exit, U_j. For axial distances $x/D > 16$, the excess centerline velocity decreases inversely with axial distance. An x^{-1} dependence in centerline velocity decay is consistent with the velocity decay measured in the near-field region of jets into still air,[25] nonreacting isothermal jets,[3] and heated jets with coflowing air[4] and corresponds to established scaling laws for the centerline velocity decay in the strong-jet limit ($u_{cl} \gg u_{co}$) over the range of axial distances studied.

Velocity Fluctuations

The centerline variation in conditional axial velocity fluctuations (normalized by the centerline excess velocity U_{cl}) is shown in Fig. 5. In general, the axial velocity fluctuations increase rapidly downstream of the jet exit to a maximum value of approximately 27% and remain nearly constant for $x/D > 35$. An asymptotic approach to a constant downstream value for the centerline velocity fluctuations has been measured in both constant-[25] and variable-density[7] turbulent jets and is consistent with the generally accepted mechanism of energy transport from the mean flow motion to turbulent energy. That is, production of turbulent energy is primarily due to the mean velocity gradient in the axial direction. The mean velocity gradient is highest near the jet exit and results in a rapid increase in the axial velocity fluctuations. Farther downstream, the mean velocity gradient decreases, and turbulent energy production is balanced by losses due to viscous dissipation and redistribution of turbulent energy to radial and tangential velocity components. This redistribution occurs through the interaction between pressure and local velocity gradient terms in the turbulent energy transport equation. Thus, $(\overline{u'^2})^{1/2}/U_{cl}$ approaches a constant asymptotic down-

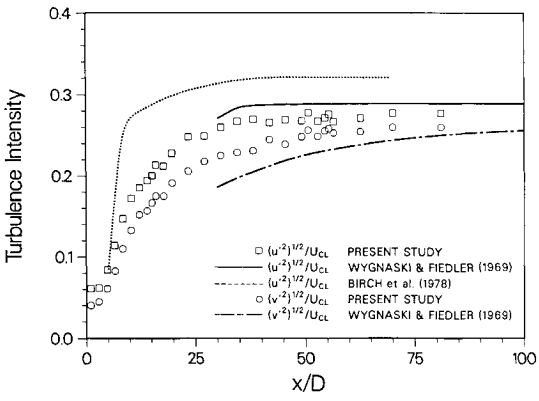

Fig. 7 Centerline variation in axial and radial velocity fluctuations □, ⊙ present study: □, axial velocity; ⊙, radial velocity; ——, Birch et al. axial velocity (CH_4 jet); ——, Wygnanski and Fiedler axial velocity (air jet); ——, Wygnanski and Fiedler radial velocity (air jet).

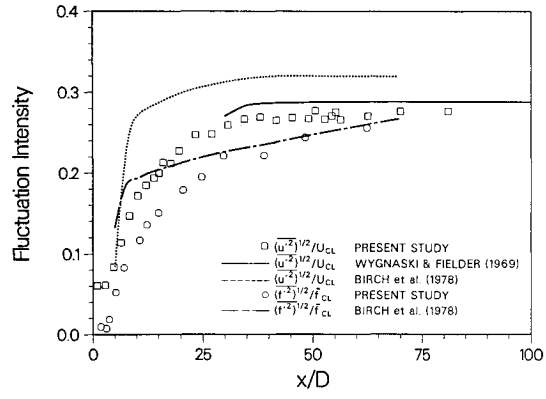

Fig. 8 Centerline variation in fluctuation intensities. □, present study axial velocity; ⊙, Schefer and Dibble mixture fraction (C_3H_8 jet); ——, Birch et al. axial velocity (CH_4 jet); ——, Birch et al. mixture fraction (CH_4 jet); ——, Becker et al. mixture fraction (air jet).

stream value determined by the balance between these production and loss terms.

Near the jet exit, axial velocity fluctuations conditional on the air are higher than those conditional on the jet. This is not unexpected since fluid originating from the airstream must be transported through a highly turbulent mixing zone located between the central jet and the coflowing air before reaching the centerline. Fluid originating from the coflowing air would therefore be characterized by a higher turbulence level. At downstream locations ($x/D > 35$), the differences in conditional axial velocity fluctuations become negligible owing to the high rates of turbulent energy transport relative to rates of change in the mean flow distribution.

The radial velocity fluctuations (Fig. 6) exhibit a similar behavior; an initially rapid increase, followed by an asymptotic approach to a constant downstream value. A comparison with Fig. 5 shows that radial velocity fluctuations increase less rapidly than axial velocity fluctuations in the region immediately downstream of the jet exit. The radial velocity fluctuations conditional on the air are also higher than those conditional on the jet fluid. However, while differences in the conditional axial velocity fluctuations become negligible for $x/D > 35$, differences in the radial velocity fluctuations are maintained for axial distances as far as 80 diameters downstream. These measurements are consistent with the observations of Wygnanski and Fiedler[25] in a self-preserving air jet; they found that radial velocity fluctuations tend to equilibrate more slowly than axial velocity fluctuations. These results were explained in terms of a stepwise turbulent energy transfer mechanism in which momentum is transferred directly from the mean flow motion to the axial velocity fluctuations. Subsequent energy transfer to the radial velocity component occurs through the interaction between pressure and local velocity gradients, which redistributes the energy among the various velocity components only after a balance is reached between the mean and fluctuating axial velocity.

Figure 7 shows a comparison between the present results and the self-preserving air jet data of Wygnanski and Fiedler.[25] Also shown are the axial velocity fluctuations measured by Birch et al.[7] in a CH_4 jet into still air. The results shown for the C_3H_8 jet were obtained with LV particles added to the jet stream only, i.e., conditional on fluid originating from the jet. This case provides a better comparison with conventionally averaged statistics since the average data rate on the centerline with LV seed added to the jet is approximately a factor of 3 higher than with LV seed added to the coflowing air. Conventionally averaged centerline values in the present study would therefore be more heavily weighted toward measurements conditional on fluid originating from the jet. In all cases shown, the axial velocity fluctuation intensity $\overline{(u'^2)}^{\frac{1}{2}}/U_{cl}$ undergoes a rapid initial increase downstream of the potential core region before asymptotically approaching a constant downstream value. The limiting downstream values for the jets shown, however, vary considerably. The present results give an asymptotic centerline value for axial velocity fluctuations of 27%, which is less than Wygnanski and Fiedler's generally accepted value of 29% for self-preserving constant-density jets.

The axial velocity fluctuations measured in the CH_4 jet ($\rho_{CH_4}/\rho_{air} = 0.55$) increase more rapidly downstream of the jet and approach a considerably higher value of 32%. The authors conclude from these results that the asymptotic limiting value for the axial velocity fluctuations is dependent on the jet-to-surrounding-fluid density ratio. The results of Birch et al.[7] are in good agreement with the velocity measurements of Antonia and Bilger[4] in a heated air jet into coflowing air ($\rho_0/\rho_{air} = 0.66$), where a limiting downstream value for $\overline{(u'^2)}^{\frac{1}{2}}/U_{cl}$ of 31% was obtained. An inverse-dependence of the limiting centerline value is therefore implied, and the limiting value for axial velocity fluctuations in the C_3H_8 jet ($\rho_{C_3H_8}/\rho_{air} = 1.52$) should fall below the constant-density airjet value. The present results verify this conclusion since our limiting value of 27% falls below the value of 29% reported by Wygnanski and Fiedler.

A comparison can also be made between the centerline behavior of axial velocity fluctuations and mixture fraction fluctuations (mixture fraction f is defined as the mass fraction of fluid originating from the central jet). The axial velocity fluctuations $\overline{(u'^2)}^{\frac{1}{2}}/U_{cl}$ measured here are replotted in Fig. 8, where they are indicated by open squares. Shown for comparison are the corresponding values for $\overline{(f'^2)}^{\frac{1}{2}}/\bar{f}_{cl}$ (indicated by open circles) obtained in the present C_3H_8 jet under identical inlet conditions.[21] While the velocity fluctuations increase rapidly and approach a constant downstream value within 35 diameters, the concentration fluctuations increase more slowly with axial distance and continue to increase up to 70 diameters downstream, where they become comparable to the velocity fluctuations. The corresponding results of Birch et al.[7] for a CH_4 jet (also shown) indicate a considerably more rapid initial increase in both $\overline{(u'^2)}^{\frac{1}{2}}/U_{cl}$ and $\overline{(f'^2)}^{\frac{1}{2}}/\bar{f}_{cl}$. In agreement with the present results, the velocity fluctuations rapidly approach a constant downstream value while the mixture fraction fluctuations continue to increase with axial distance at a rate comparable to the present C_3H_8 jet and show good agreement with the present results for $x/D > 30$.

While the present results and those of other studies generally show that centerline velocity fluctuations asymptotically approach a constant downstream, the question of whether the mixture fraction fluctuations exhibit the same behavior has

not been satisfactorily resolved. The centerline variation in mixture fraction fluctuations has recently been studied by Pitts,[16] who used laser-Rayleigh scattering to investigate the effects of variable density on the mixing behavior of turbulent axisymmetric jets. Extensive comparisons were made with previous findings in the literature. While all studies showed an initially rapid increase in mixture fraction fluctuations downstream of the potential core region, the behavior at distances beyond the region of rapid rise was less consistent. Some studies showed that the fluctuations attained a constant downstream value, while others showed that the fluctuations continued to increase with downstream distance. A qualitative explanation for these seemingly contradictory results was suggested, based on Reynolds number and density differences between experimental studies. Pitts speculated that the downstream distance required to attain asymptotic downstream behavior increases with the jet density and Reynolds number (this explanation is in qualitative agreement with the trends observed here). Thus, many experimental measurements, particularly those obtained in high Reynolds number jets, are not taken far enough downstream for asymptotic behavior to be fully attained. Clearly, further experimental work is needed to verify the effect of density variations on the downstream behavior of turbulence quantities and the reason for the apparent differences in limiting asymptotic values. The data presented here do, however, indicate that the limiting centerline value for the velocity fluctuations shows greater sensitivity to jet density than the corresponding concentration fluctuations.

Radial Profiles

Mean Velocity

Radial profiles of the mean axial and radial velocity are shown in Fig. 9 at an axial location of $x/D = 30$. The mean axial velocity, presented as excess velocity $\bar{U} = \bar{u} - \bar{u}_{co}$, is shown in Fig. 9a. Fluid originating from the jet is moving at a higher velocity than fluid originating from the slower-moving coflow air across most of the jet. The mean velocity conditional on the jet is approximately 4% greater than the velocity conditional on the air at the centerline (corresponding to an absolute velocity difference of 1 m/s) and increases to nearly 10% at the outermost radial location (where the absolute velocity difference has increased to approximately 2 m/s). These results are consistent with results in other turbulent shear flows, where conditional measurements indicate significant differences in turbulent and nonturbulent zone statistics in the outer mixing layer.[5,8]

Conditional measurements of the radial velocity component, $\bar{v}_{\text{air}}$ and $\bar{v}_{\text{jet}}$, are presented in Fig. 9b. In the sign convention adopted for the radial velocity, a positive value indicates flow outward from the centerline, while a negative value corresponds to flow toward the centerline. The higher values of $\bar{v}_{\text{jet}}$ correspond to more rapid outward flow of high-velocity fluid originating from the region near the centerline. The absolute differences in radial velocity are smallest near the centerline, where symmetry requires that the mean radial velocity goes through zero and increases to a maximum of approximately 1 m/s in the mixing region ($y/D > 2$). At the outermost radial locations, fluid originating from the jet continues to move outward, while the negative values of $\bar{v}_{\text{air}}$ indicate inward flow of entrained fluid from the coflowing airstream.

Velocity Fluctuations

Radial profiles of the normalized axial velocity fluctuations $\overline{(u'^2)}^{\frac{1}{2}}_{\text{jet}}/U_{cl}$ and $\overline{(u'^2)}^{\frac{1}{2}}_{\text{air}}/U_{cl}$ are shown in Fig. 9c. The fluctuations conditional on both the jet and the air are nearly the same at the centerline, which is consistent with the centerline profiles presented previously. The value of $\overline{(u'^2)}^{\frac{1}{2}}_{\text{air}}/U_{cl}$ increases to a maximum of approximately 26% in the mixing region before decreasing rapidly in the outer part of the jet ($y/D > 2$) to a level corresponding to that of the coflowing air. This behavior is in contrast to $\overline{(u'^2)}^{\frac{1}{2}}_{\text{jet}}/U_{cl}$, which remains relatively constant across the mixing layer and decreases less rapidly in the outer region of the jet. The higher fluctuations in fluid originating from the jet at large radii are explained by the fact that jet fluid at these locations has, on average, emerged from the centerline region, which is generally more turbulent, and has had insufficient time to equilibrate fully with lower-turbulence fluid originating from the coflowing air.

Corresponding profiles of the radial velocity fluctuations are shown in Fig. 9d. The radial velocity fluctuations conditional on the air are higher across the central region of the jet for $y/D < 2$. Analogous to the axial velocity fluctuations, $\overline{(v'^2)}^{\frac{1}{2}}_{\text{air}}/U_{cl}$ decreases more rapidly than $\overline{(v'^2)}^{\frac{1}{2}}_{\text{jet}}/U_{cl}$ for radial distances $y/D > 2$. The decrease in $\overline{(v'^2)}^{\frac{1}{2}}_{\text{jet}}/U_{cl}$ is less rapid than the corresponding axial velocity fluctuations and results in a noticeably greater difference between conditional radial velocity fluctuations in the outer region of the jet. These results again show that the radial velocity fluctuations equilibrate less rapidly than the axial velocity fluctuations and are in agreement with measurements along the centerline.

The correlation between the fluctuating components of radial and axial velocities, presented in Fig. 9e, is directly related to the turbulent transport of momentum. Both $\overline{u'v'}_{\text{jet}}/U_{cl}^2$ and $\overline{u'v'}_{\text{air}}/U_{cl}^2$ reach a maximum in the mixing region between the fuel jet and the outer airflow. The values of $\overline{u'v'}_{\text{jet}}/U_{cl}^2$ are greater for $y/D > 2$, which emphasizes the role of highly turbulent jet fluid momentum transport in the outer regions of the jet. Across the central region of the jet, for $y/D < 2$, $\overline{u'v'}_{\text{air}}/U_{cl}^2$ is greater than $\overline{u'v'}_{\text{jet}}/U_{cl}^2$. This result is not unexpected owing to the generally higher turbulent fluctuations (see Figs. 9c and 9d) associated with previously entrained air, which has been transported from outer flow regions across the mixing region toward the centerline.

From the above results, it can be seen that the greatest differences in conditional statistics for both velocity components occur 1) along the centerline in the mixing region located immediately downstream of the jet potential core, where a significant difference between centerline and coflow air velocity still exists, and 2) in the mixing region between the high-velocity central jet and the outer coflowing air. In both regions, insufficient time is available for fluid originating from the jet and the coflowing air to become "fully mixed" with respect to momentum transfer. The greater differences in the radial velocity statistics in these regions indicate a longer mixing-time requirement for the radial velocity component to reach equilibrium and can be explained in terms of the stepwise energy transfer mechanism discussed previously.

Similarity Considerations

Radial velocity profiles were measured at several axial locations to determine the variation of conditional statistics and the growth of the mixing region with downstream distance. Figure 10 shows the radial variation in conditional velocity statistics at three axial locations, $x/D = 15$, 30, and 50. The downstream flow development of axisymmetric turbulent jets is typically described in terms of similarity variables (see e.g., Hinze[12]). Three flow regimes can generally be identified as a function of downstream distance. These include: 1) an upstream potential core region limited to within several jet diameters of the jet exit, 2) a flow development region in which the flow develops the characteristics that eventually lead to 3) a downstream region in which the flow attains truly self-similar behavior. The later regime typically occurs far downstream; for instance, self-similar behavior was found only for $x/D > 140$ in Wygnanski and Fielder's widely quoted air jet study. Measurements by other workers have shown that local similarity can occur sooner than the distance required for exact similarity (e.g., truly self-preserving flow) to be established.[16] While it is recognized that the effects of coflow

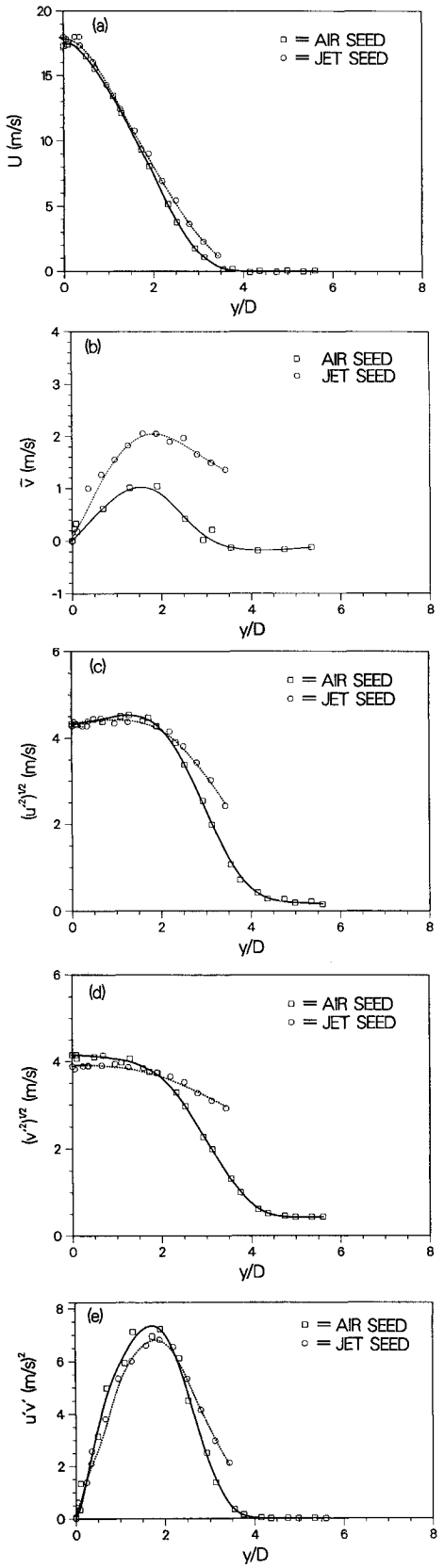

Fig. 9 Radial profiles for a turbulent nonreacting propane jet at an axial location of $x/D = 30$. Bulk jet velocity = 53 m/s; coflowing air velocity = 9.2 m/s. Solid line indicates data collected with LDV seed added to the coflowing airstream only; dotted line indicates data collected with LDV seed added to the propane jet stream only; □, coflowing air seed only; ⊙, jet seed only. a) Radial profiles of mean axial velocity; b) radial profiles of mean radial velocity; c) radial profiles of axial velocity fluctuations; d) radial profiles of radial velocity fluctuations; e) radial profiles of axial and radial velocity correlation.

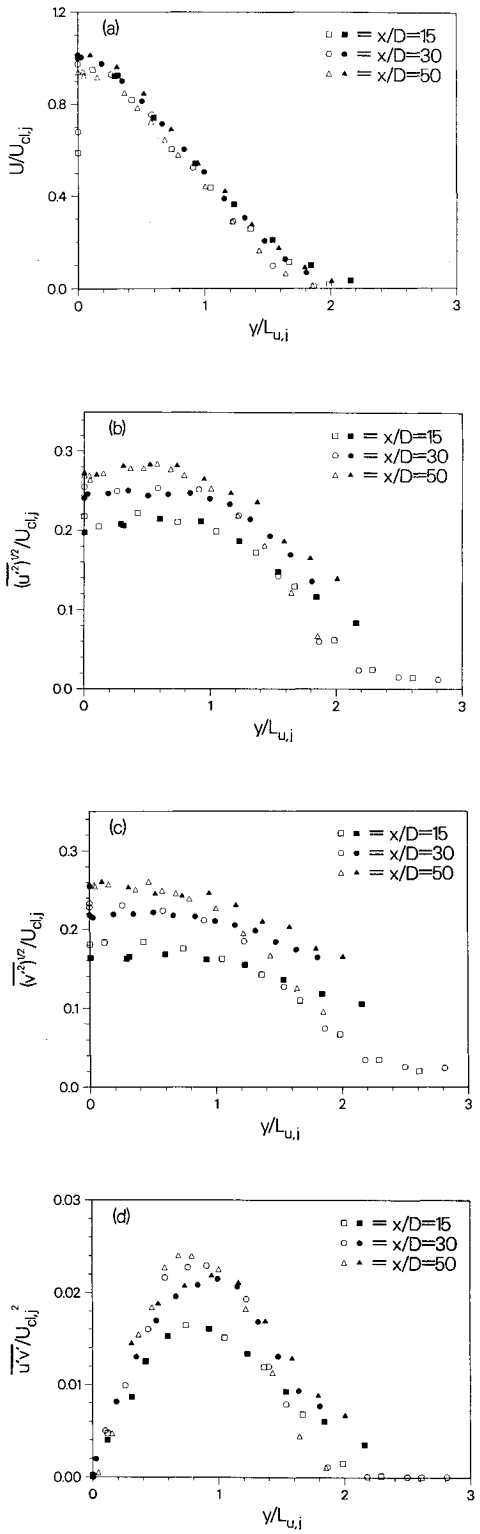

Fig. 10 Normalized radial profiles for a turbulent nonreacting propane jet at axial locations of $x/D = 15$, 30, and 50. Bulk jet velocity = 53 m/s; coflowing air velocity = 9.2 m/s. Solid line indicates data collected with LDV seed added to the coflowing airstream only; dotted line indicates data collected with LDV seed added to the propane jet stream only; open symbols, coflowing air seed only; solid symbols, jet seed only. a) Radial profiles of mean axial velocity; b) radial profiles of axial velocity fluctuations; c) radial profiles of radial velocity fluctuations; d) radial profiles of axial and radial velocity correlation.

Table 1 Centerline excess velocity and velocity half-radius

	Jet seed		Air seed	
x/D	U_{cl} (m/s)	L_u/D	U_{cl} (m/s)	L_u/D
15	35.3	0.98	33.2	0.90
30	17.8	1.88	17.3	1.78
50	10.4	2.84	9.6	2.48

air and variable density prevent such flows from attaining true similarity, the present results are shown in terms of local similarity variables to facilitate comparisons with data obtained in other jets and to emphasize the development of radial variations in conditional velocity statistics. A flow is considered to be locally similar when the velocity (or concentration) profiles can be collapsed in terms of local geometric variables. The appropriate variables for the present study are the radial distance normalized by the velocity half-radius L_u (defined as the radial location at which the excess velocity is equal to half its centerline value) and the velocity normalized by the centerline excess velocity U_{cl}. Values of L_u and U_{cl} based on data obtained with seed added to only the jet and only the coflowing air are shown in Table 1. For the results shown in Fig. 10, L_u and U_{cl} are based only on measurements conditional on the jet to further emphasize differences between the conditional statistics.

Radial profiles of the normalized mean axial velocity (presented as excess velocity) are shown in Fig. 10a. The axial velocity profiles conditional on the jet and on the air show local similarity within the first 15 jet diameters. For a given radial location, the velocity conditional on the jet is higher than the corresponding value conditional on the air at all axial locations. In addition, the magnitude of the difference remains nearly constant across the jet and is comparable at all three axial locations, indicating that the conditional velocity difference scales with the centerline excess velocity.

Profiles of the normalized axial and radial velocity fluctuations $\overline{(u'^2)}^{\frac{1}{2}}/U_{cl}$ and $\overline{(v'^2)}^{\frac{1}{2}}/U_{cl}$ and their correlation $\overline{u'v'}/U_{cl}^2$ are shown in Figs. 10b–10d, respectively. In general, the radial variation in conditional statistics at all axial locations is qualitatively similar; differences are relatively small near the centerline, where the fluid is well mixed, and increase to a maximum in the outer mixing region. Neither the profiles conditional on the jet or on the air show similarity over the range of axial distances studied. Comensurate with the mean axial velocity measurements, the absolute differences in conditional results (at a given radial location) are comparable at all axial locations and again indicate that differences in the conditional velocity statistics scale with the centerline excess velocity. These observations imply a similar mixing history for the jet fluid and entrained air, which is independent of downstream distance.

Probability Density Distributions

Probability density distributions of the axial velocity conditional on the jet fluid $p(u)_{\text{jet}}$ and on the air $p(u)_{\text{air}}$ are shown in Fig. 11 for $x/D = 30$ and various distances from the centerline. The distributions shown were calculated from 3000 velocity measurements at each spatial location using 30 bins equally spaced over the 3 sigma limits of the data. As in the previous section, the solid line indicates data conditional on the air and the dotted line indicates data conditional on the jet fluid.

The axial velocity distributions are, in general, characterized by a unimodal distribution, which shifts to a higher average velocity as the centerline is approached. In the outer mixing

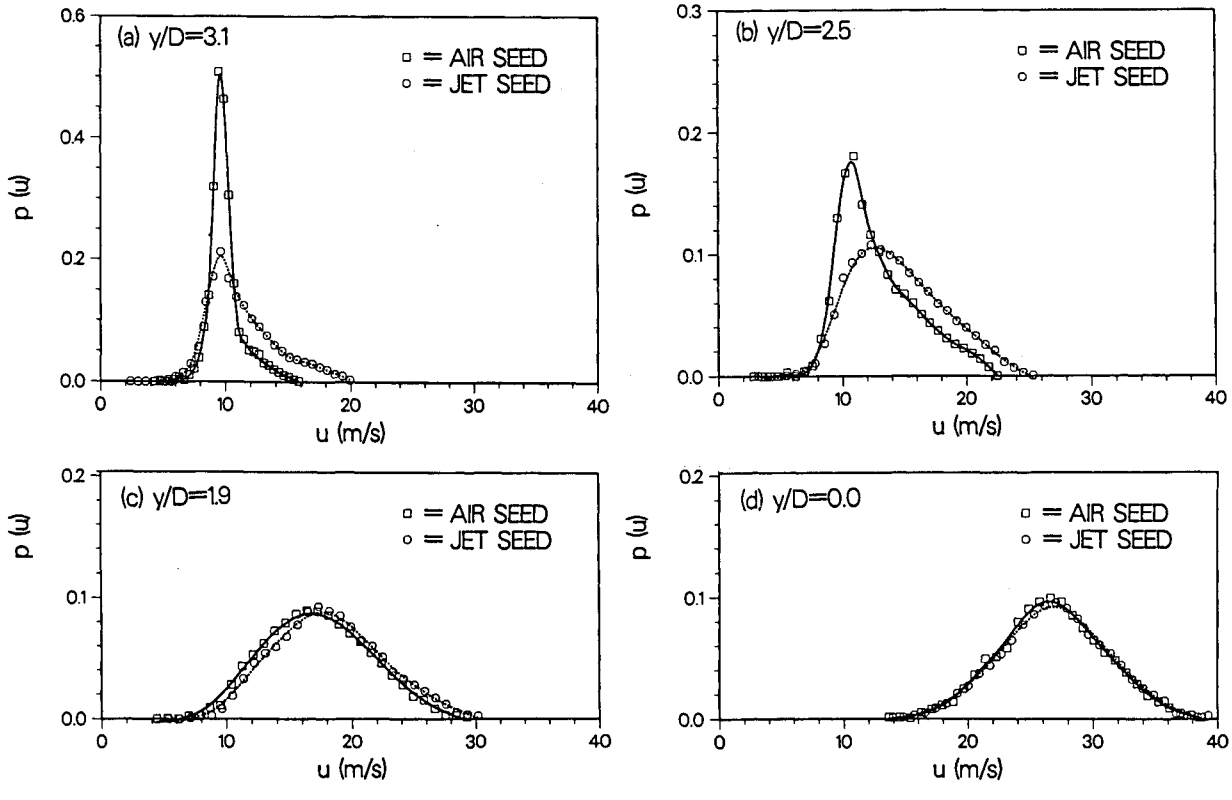

Fig. 11 Conditionally sampled probability density distributions of axial velocity for a turbulent nonreacting propane jet at an axial location of $x/D = 30$. Bulk jet velocity = 53 m/s; coflowing air velocity = 9.2m/s. Solid line indicated data collected with LDV seed added to the coflowing airstream only; dotted line indicates data with the LDV seed added to the jet stream only; □, coflowing air seed only; ⊙, jet seed only. a) $y/D = 3.1$; b) $y/D = 2.5$; c) $y/D = 1.9$; d) $y/D = 0.0$.

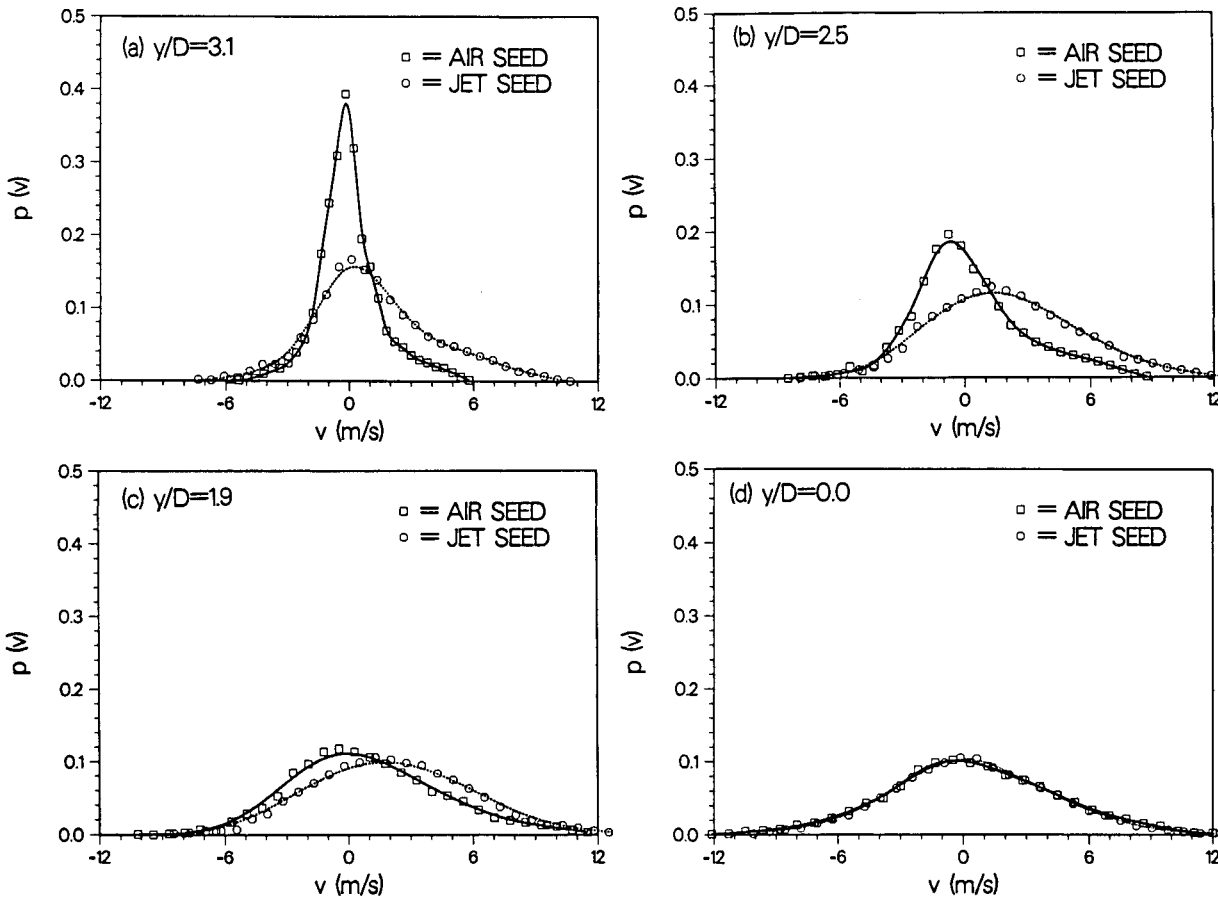

Fig. 12 Conditionally sampled probability density distributions of radial velocity for a turbulent nonreacting propane jet at an axial location of $x/D = 30$. Bulk jet velocity = 53 m/s; coflowing air velocity = 9.2 m/s. Solid line indicates data collected with LDV seed added to the coflowing airstream only; dotted line indicates data with the LDV seed added to the jet stream only; □, coflowing air seed only; ⊙, jet seed only. a) $y/D = 3.1$; b) $y/D = 2.5$; c) $y/D = 1.9$; d) $y/D = 0.0$.

region at $y/D = 3.1$, Fig. 11a, $p(u)_{air}$ is relatively narrow, with a mean velocity close to that of the coflowing air velocity. The maximum in the distribution for $p(u)_{jet}$ is located at nearly the same velocity as $p(u)_{air}$ but is clearly skewed toward higher velocities, which accounts for the higher observed mean and fluctuating axial velocities conditional on the jet. At $y/D = 2.5$, Fig. 11b, $p(u)_{air}$ shows an increasing contribution from high-velocity fluid. This high-velocity contribution is due to previously entrained air that has been partially mixed with faster-moving jet fluid originating from near the centerline. The maximum in $p(u)_{jet}$ has shifted toward higher velocities, and the distribution has broadened considerably owing to the higher turbulence levels near the centerline, where the jet fluid originates.

More complete mixing of fluid originating from the jet and the coflowing air is apparent closer to the centerline in Fig. 11c. The differences in $p(u)_{jet}$ and $p(u)_{air}$ have decreased considerably, and the distributions have taken on the more Gaussian appearance characteristic of isotropic turbulence. The width of the distributions are comparable, while the peak in $p(u)_{jet}$ is at a slightly higher velocity than $p(u)_{air}$. At the centerline, Fig. 11d, both distributions are closely Gaussian (skewness = 0.0, kurtosis = 3.0) and nearly identical. At this location, fluid originating from the jet and the airstreams is relatively well mixed.

The corresponding radial velocity distributions $p(v)_{air}$ and $p(v)_{jet}$ are shown in Fig. 12. At $y/D = 3.1$, $p(v)_{air}$ is considerably narrower than $p(v)_{jet}$. In both cases, the maximum in the distribution is centered near zero, while the presence of positive and negative radial velocities corresponds to outward flow from the centerline region and inward flow of mixed fluid originating from both the jet and the coflowing air, respectively. The positive mean values of radial velocity for both cases at this location (see Fig. 9b) indicate that the fluid, on average, is moving outward from the centerline region. The distribution $p(v)_{jet}$ shows considerably higher positive velocities than $p(v)_{air}$ at outer radial locations since fluid originating from the central jet is moving more rapidly away from the centerline. Nearly equal entrainment of fluid originating from the jet and air is indicated by the relatively small differences in $p(u)_{jet}$ and $p(u)_{air}$ at negative radial velocities.

At $y/D = 2.5$, the maximum in $p(v)_{air}$ occurs at negative radial velocities and corresponds to entrainment of coflowing air inward toward the centerline. More rapid flow of previously entrained air outward from the centerline is also indicated by the increased positive velocity contribution to $p(v)_{air}$. The maximum in $p(v)_{jet}$ is located at positive radial velocities, and the distribution is more skewed toward positive velocities. At $y/D = 1.9$, the peak in $p(v)_{air}$ at negative velocity is less pronounced although considerable entrainment of fluid originating from the airstream is still shown. More rapid flow outward from the centerline of fluid originating from the air is also shown by the general shift in $p(v)_{air}$ toward positive velocities as the centerline is approached. At the centerline, the distributions conditional on both the jet and the air are closely Gaussian and centered at zero radial velocity. The distribution $p(v)_{air}$ is slightly broader, which accounts for the higher radial velocity fluctuations measured on the centerline in fluid originating from the coflowing air.

The probability density distributions at $x/D = 15$ and 50 are qualitatively similar to those at $x/D = 30$. The flow at upstream locations is characterized by more rapid entrainment of coflowing air by the higher-velocity jet fluid and more rapid flow outward of both fluid originating from the jet and entrained air, which is mixed with the high-velocity jet fluid and subsequently expands outward.

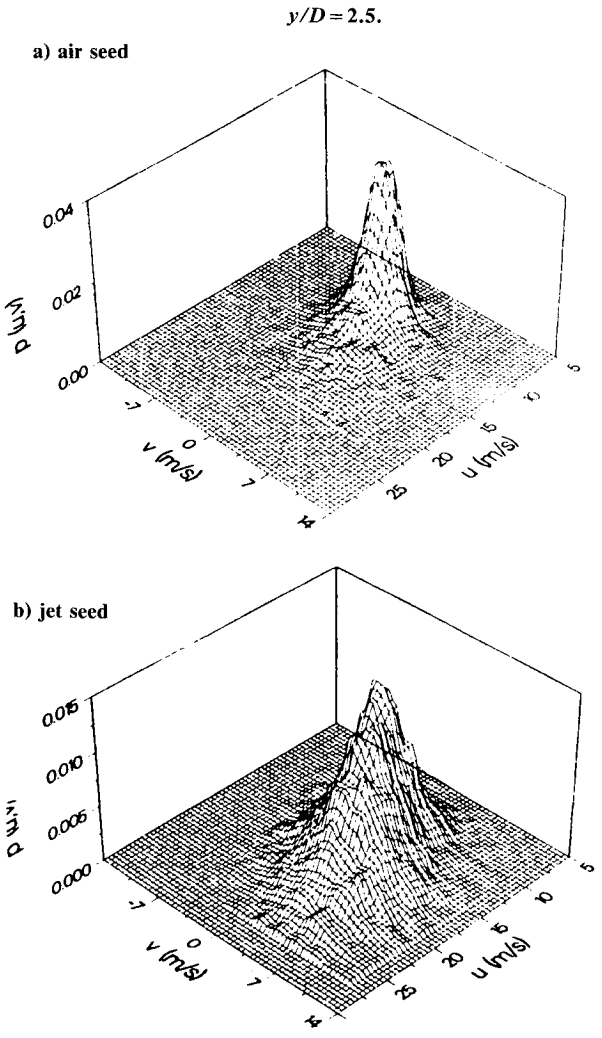

Fig. 13 Joint probability density distributions of axial and radial velocity for a turbulent nonreacting propane jet at an axial location $x/D = 30$ and a radial location of $y/D = 2.5$. a) LDV seed added to the coflowing air only; b) LDV seed added to the jet only. Bulk jet velocity = 53 m/s; coflowing air velocity = 9.2 m/s.

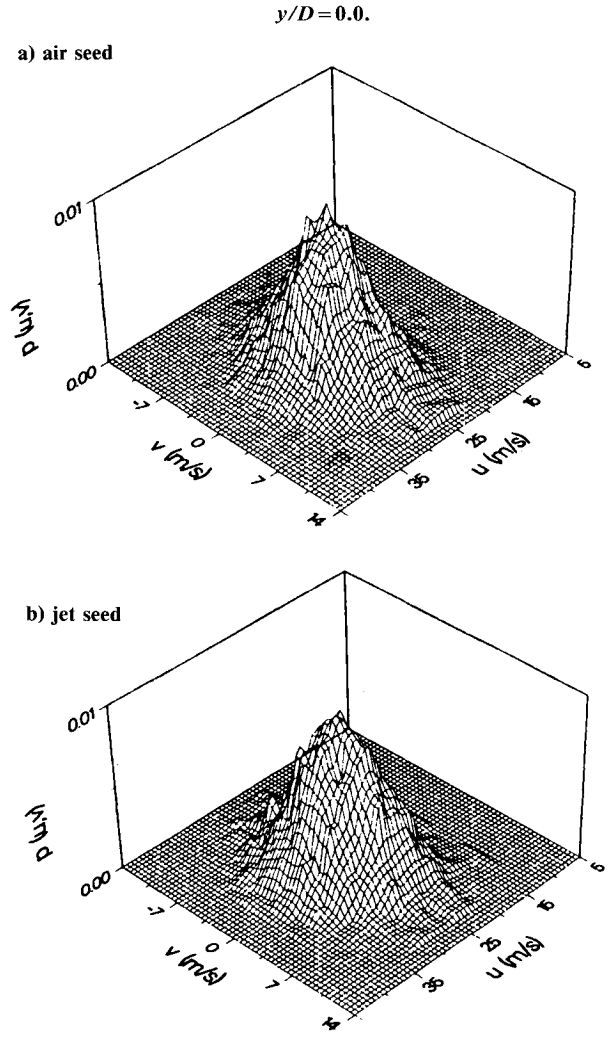

Fig. 14 Joint probability density distributions of axial and radial velocity for a turbulent nonreacting propane jet at an axial location $x/D = 30$ and a radial location of $y/D = 0.0$. a) LDV seed added to the coflowing air only; b) LDV seed added to the jet only. Bulk jet velocity = 53 m/s; coflowing air velocity = 9.2 m/s.

Joint Probability Density Distributions

Joint probability density distributions of axial and radial velocity at $x/D = 30$ are shown in Figs. 13 and 14 for radial distances of $y/D = 2.5$ and 0.0, respectively. Shown are the distributions conditional on the air $p(u,v)_{\text{air}}$ (upper figure) and on the jet $p(u,v)_{\text{jet}}$ (lower figure). The distributions were calculated from 10,000 velocity pairs at each spatial location, using 20 axial and radial velocity bins spaced over the 3 sigma limits of the data.

The distribution at $y/D = 2.5$ corresponds to the outer edge of the mixing region, where the fluid is predominantly air. The distribution conditional on the air $p(u,v)_{\text{air}}$, Fig. 13a, is characterized by a relatively narrow distribution, with the axial velocity distribution centered at a velocity near the coflowing air velocity and the radial velocity distribution centered near zero. At higher axial velocities, the radial velocity distribution is highly skewed toward positive values corresponding to the more rapid movement of higher-velocity fluid away from the centerline. The broader distribution at high axial velocities also indicates considerably higher radial velocity fluctuations associated with the faster-moving fluid. It is likely that this fluid, originating from the airstream, has been previously entrained and mixed with higher-velocity jet fluid before flowing outward toward the coflowing airstream. The primary contribution to the distribution conditional on the jet $p(u,v)_{\text{jet}}$, Fig 13b, is again from fluid moving in the axial direction at near the coflowing air velocity. A maximum exists in $p(u,v)_{\text{jet}}$ at axial velocities close to the coflowing air velocity, and considerably more rapid outward flow of the high-velocity jet fluid is apparent. The fluctuations in both axial and radial velocities are higher, as shown by the broader radial velocity distribution for the faster-moving fluid. This observation corresponds to the higher axial and radial velocity fluctuations seen in Fig. 9.

At the centerline, Fig. 14, the low velocity peak in $p(u,v)_{\text{air}}$ (top) is no longer present, and both $p(u,v)_{\text{air}}$ and $p(u,v)_{\text{jet}}$ have become more generally Gaussian and are centered at a higher mean axial velocity and zero radial velocity. As observed in the previous section, the distributions for both cases are nearly identical since sufficient mixing between the jet stream and airstream has occurred. Flow outward from the centerline in both directions is apparent, but the predominant flow direction, as indicated by the peak in the distributions, is along the centerline.

The relationship between radial and axial velocities at $x/D = 30$ is shown more clearly in Figs. 15 and 16. Here the probability density distributions for radial velocity at various axial velocities are shown. At $y/D = 2.5$, the distributions at low axial velocities conditional on the air, Fig. 15a, are relatively narrow and are centered at negative radial velocities

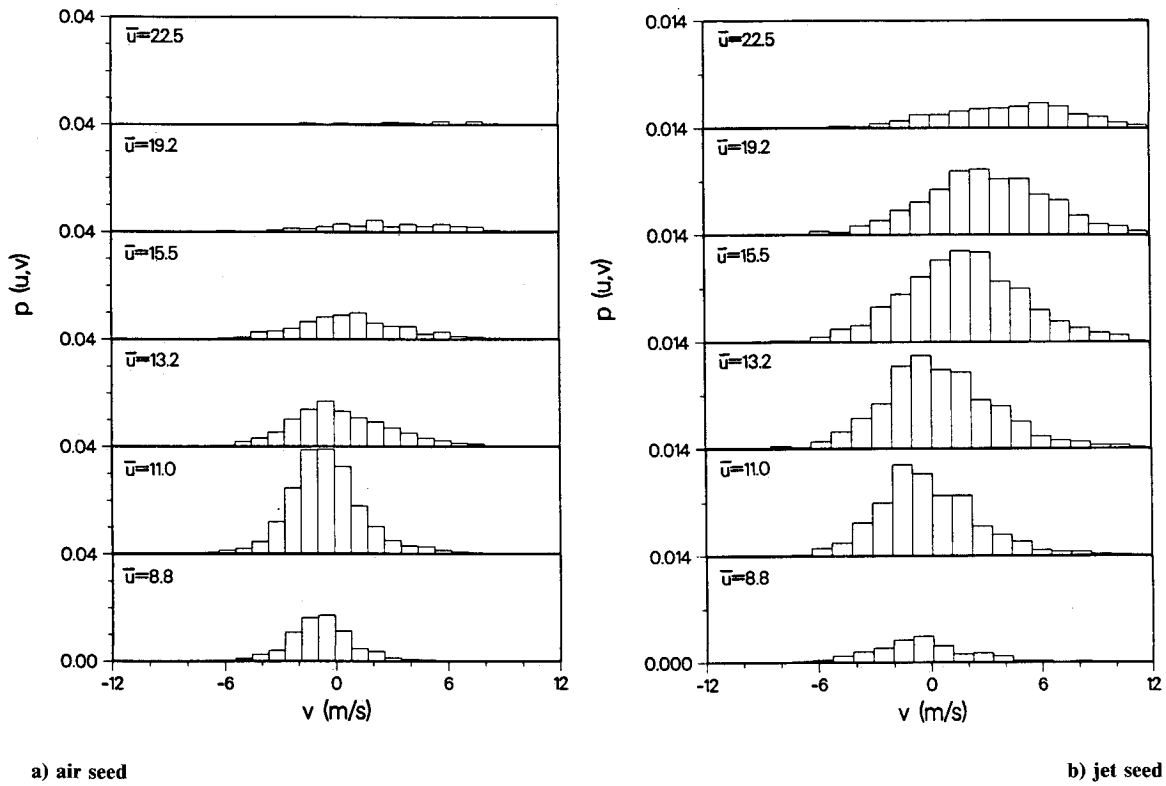

Fig. 15 Joint probability density distributions of axial and radial velocity for a turbulent nonreacting propane jet at an axial location $x/D = 30$ and a radial location of $y/D = 2.5$. a) LDV seed added to the coflowing air only; b) LDV seed added to the jet only. Bulk jet velocity = 53 m/s; coflowing air velocity = 9.2 m/s.

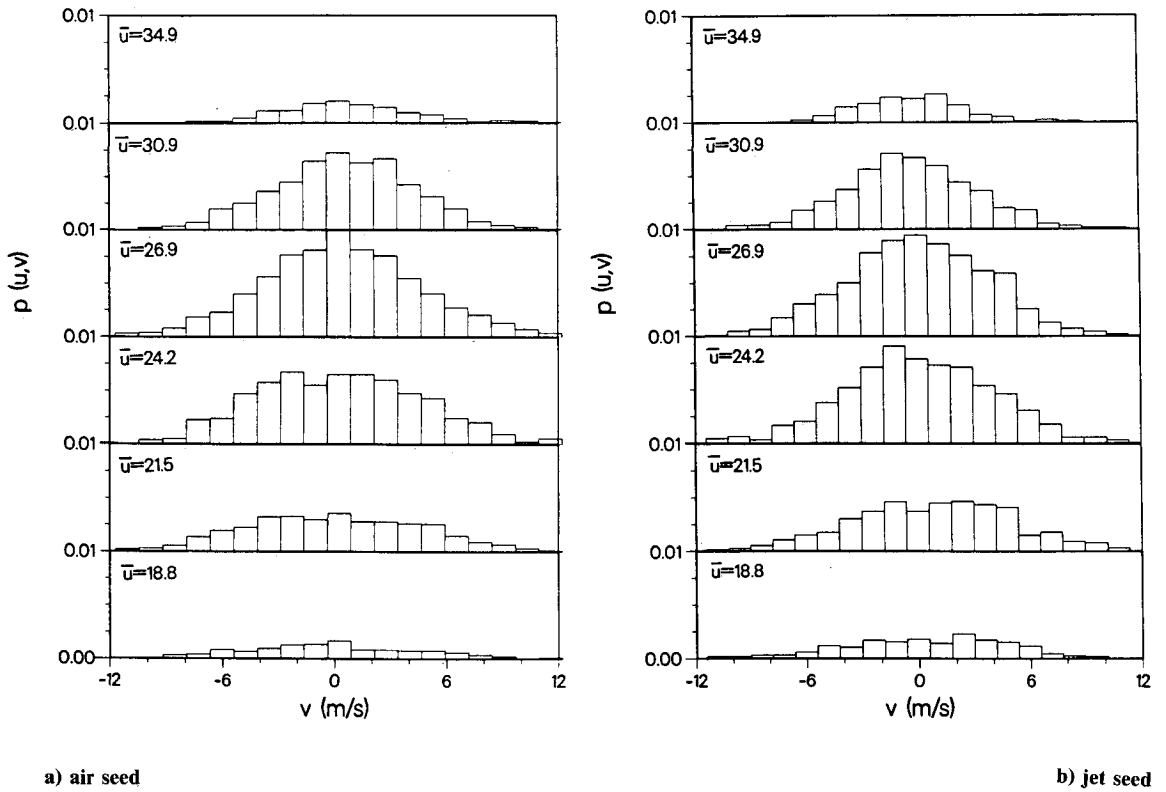

Fig. 16 Joint probability density distributions of axial and radial velocity for a turbulent nonreacting propane jet at an axial location $x/D = 30$ and a radial location of $y/D = 0.0$. a) LDV seed added to the coflowing air only; b) LDV seed added to the jet only. Bulk jet velocity = 53 m/s; coflowing air velocity = 9.2 m/s.

corresponding to the entrainment of lower-velocity air toward the centerline. At higher axial velocities, the distributions shift toward positive radial velocities as coflowing air is entrained by the jet fluid, undergoes mixing with high-velocity fluid originating near the centerline, and subsequently expands outward. The distributions conditional on the jet, Fig. 15b, are qualitatively similar. Fluid moving at lower axial velocities generally undergoes greater entrainment, while faster-moving jet fluid is characterized by more rapid outward flow.

At the centerline, Figs. 16a and 16b, the radial velocity distributions conditional on both the air and jet can best be described as nearly Gaussian and centered at a radial velocity near zero.

Results at $x/D = 50$ (not shown) are similar to those described above at $x/D = 30$, with the exception, as mentioned previously, that the flow at upstream locations, i.e., $x/D = 30$, is characterized by more rapid entrainment of coflowing air by the high-velocity jet fluid and more rapid flow outward of the jet fluid. In general, the above observations indicate that the motion of the jet fluid is primarily characterized by flow outward from the centerline, where it mixes with slower-moving air, and entrainment of coflowing air inward, where mixing occurs with high-velocity jet fluid. Both entrainment of fluid originating in the airstream and outward flow of the jet fluid are more rapid at upstream locations.

Summary and Conclusions

A two-color LV system has been used to measure simultaneously the axial and radial components of velocity in a turbulent, variable-density propane jet. Conditional statistics have been obtained by alternately seeding only the jet fluid and the coflowing air.

Measured values of velocity fluctuations along the jet centerline show that 1) the asymptotic approach to a steady-state downstream value is more rapid for the axial velocity fluctuations than for the radial velocity fluctuations and 2) the radial velocity fluctuations asymptotically approach a lower downstream value. This is consistent with measurements in self-preserving constant-density air jets, where it has been concluded that radial velocity fluctuations tend to equilibrate more slowly than axial velocity fluctuations.

The asymptotic, limiting-downstream value for centerline axial velocity fluctuation intensity in the present C_3H_8 jet is 27%. This value falls below the 29% value measured in a self-preserving air jet. In contrast, the fluctuation intensity measured in a CH_4 jet approaches a considerably higher value of 32%. These results indicate an inverse dependence of centerline velocity fluctuation intensity on the jet-to-surrounding-fluid density ratio.

The greatest differences in conditional statistics for both velocity components are observed in 1) the mixing region along the centerline and downstream of the potential core region and in 2) the mixing region between the high-velocity central region of the jet and the outer coflowing air. It is likely that in both regions, insufficient time is available for fluid originating from the jet and the coflowing air to become fully mixed with respect to momentum transfer. The greater differences in the conditional mean and fluctuating radial velocity along the centerline and at outer radial locations indicate a longer mixing-time requirement for the radial velocity component. These results indicate a stepwise momentum transfer mechanism in which momentum is transferred directly from the mean flow motion to the axial velocity fluctuations and, only after a balance is reached between the mean and fluctuating axial velocity, does further transfer to the radial velocity component occur through the pressure and velocity gradient terms in the momentum equation.

The conditional probability density distributions of velocity show that the motion of the jet fluid is primarily characterized by flow outward from the centerline, where it mixes with slower-moving air, and entrainment of coflowing air toward the centerline, where mixing occurs with high-velocity jet fluid. Re-entrainment of jet fluid that has previously mixed with coflowing air, as well as outward flow of previously entrained air, is also indicated.

Acknowledgments

This research was supported by the U.S. Department of Energy, Office of Basic Energy Sciences, Division of Chemical Sciences.

References

[1]Antonia, R.A., "Conditional Sampling in Turbulence Measurement," *Annual Review of Fluid Mechanics*, Vol. 13, 1981, pp. 131–156.

[2]Antonia, R.A., "Conditionally Sampled Measurements Near the Outer Edge of a Turbulent Boundary Layer," *Journal of Fluid Mechanics*, Vol 56, 1972, pp. 1–18.

[3]Antonia, R.A. and Bilger, R.W., "An Experimental Investigation of an Axisymmetric Jet in a Co-flowing Air Stream," *Journal of Fluid Mechanics*, Vol. 64, Pt. 4, 1973, pp. 805–822.

[4]Antonia, R.A. and Bilger, R.W., "The Heated Jet in a Coflowing Air Stream," *AIAA Journal*, Vol. 14, Nov. 1976, pp. 1541–1547.

[5]Antonia, R.A., Prabhu, A., and Stephenson, S.E., "Conditionally Sampled Measurements in a Heated Turbulent Jet," *Journal of Fluid Mechanics*, Vol. 72, 1975, pp. 455–480.

[6]Bilger, R.W. and Dibble, R.W., "Differential Molecular Diffusion Effects in Turbulent Mixing," *Combustion Science and Technology*, Vol. 28, 1982, pp. 161–169.

[7]Birch, A.D., Brown, D.R., Dodson, M.G., and Thomas, J.R., "The Turbulent Concentration Field of a Methane Jet," *Journal of Fluid Mechanics*, Vol. 88, 1978, pp. 431–449.

[8]Chevray, R. and Tutu, N.K., "Intermittency and Preferential Transport of Heat in a Round Jet," *Journal of Fluid Mechanics*, Vol. 88, Pt. 1, 1978, pp. 138–160.

[9]Corrsin, S. and Kistler, A.L., "Free-stream Boundaries of Turbulent Flows," NACA Rept. 1244, 1955.

[10]Dibble, R.W., Hartmann, V., Schefer, R.W., and Kollmann, W., "Conditional Sampling of Velocity and Scalars in Turbulent Flames Using Simultaneous LDV-Raman Scattering," *Journal of Experimental Fluids*, Vol. 5, 1987, pp. 103–113.

[11]Durst, F., Melling, A., and Whitelaw, J.A., *Principles and Practice of Laser-Doppler Anemometry*, Academic Press, London, England, 1976.

[12]Hinze, J.O., *Turbulence*, McGraw-Hill, New York, 1975.

[13]Kollmann, W., "The Prediction of the Intermittency Factor for Turbulent Shear Flows," AIAA Paper 83-0382, 1983.

[14]Libby, P.A., "On the Prediction of Intermittent Turbulent Flows," *Journal of Fluid Mechanics*, Vol. 68, Pt. 2, 1975, pp. 273–295.

[15]McLaughlin, D.K. and Tiederman, W.G., "Biasing Correction for Individual Realization of Laser Anemometer Measurements in Turbulent Flows," *Physics of Fluids*, Vol. 16, 1973, pp. 2082–2085.

[16]Pitts, W.M., "Effects of Global Density and Reynolds Number Variations on Mixing in Turbulent, Axisymmetric Jets," National Bureau of Standards Report NBSIR 86-3340, March 1986.

[17]Pitz, R.W. and Drake, M.C., "Intermittency and Conditional Averaging in a Turbulent Nonpremixed Flame by Raman Scattering," AIAA Paper 84-0197, 1984.

[18]Pope, S.B., "Calculations of a Plane Turbulent Jet," AIAA Paper 83-0286, Jan. 1983.

[19]Razdan, M.K. and Stevens, J.G., "CO/Air Turbulent Diffusion Flame: Measurements and Modeling," *Combustion and Flame*, Vol. 59, 1985, pp. 289.

[20]Schefer, R.W., Johnston, S.C., Dibble, R.W., Gouldin, F.C., and Kollmann, W., "Nonreacting Turbulent Mixing Flows: A Literature Survey and Data Base," Sandia National Laboratories, Livermore, CA, Sandia Rept. SAND86-8217, 1986.

[21]Schefer, R.W. and Dibble, R.W., "Mixture Fraction Measurements in a Turbulent Nonpremixed Propane Jet," AIAA Paper 86-0278, 1986.

[22]Schefer, R.W. and Dibble, R.W., "Simultaneous Measurements of Velocity and Density in a Turbulent Nonpremixed Flame," *AIAA Journal*, Vol. 23, July 1985, pp. 1070–1078.
[23]Strahle, W.C. and Lekoudis, S.G. (eds.), "Evaluation of Data on Simple Turbulent Reacting Flows," AFOSR Rept. TR-85 0880, Sept. 1985.
[24]Warshaw, S., Lapp, M., Penney, C.M., and Drake, M.D., "Temperature-Velocity Correlation Measurements for Turbulent Diffusion Flames from Vibrational Raman-Scattering Diagnostics," *Laser Probes for Combustion Chemistry*, edited by D.R. Crosley, Paper 19, American Chemical Society Symposium Series, Vol. 134, 1980, pp. 239–246.
[25]Wygnanski, I. and Fiedler, H., "Some Measurements in the Self-preserving Jet," *Journal of Fluid Mechanics*, Vol. 38, Pt. 3, 1969, pp. 577–612.

From the AIAA Progress in Astronautics and Aeronautics Series

THERMOPHYSICS OF ATMOSPHERIC ENTRY—v. 82

Edited by T.E. Horton, The University of Mississippi

Thermophysics denotes a blend of the classical sciences of heat transfer, fluid mechanics, materials, and electromagnetic theory with the microphysical sciences of solid state, physical optics, and atomic and molecular dynamics. All of these sciences are involved and interconnected in the problem of entry into a planetary atmosphere at spaceflight speeds. At such high speeds, the adjacent atmospheric gas is not only compressed and heated to very high temperatures, but stongly reactive, highly radiative, and electronically conductive as well. At the same time, as a consequence of the intense surface heating, the temperature of the material of the entry vehicle is raised to a degree such that material ablation and chemical reaction become prominent. This volume deals with all of these processes, as they are viewed by the research and engineering community today, not only at the detailed physical and chemical level, but also at the system engineering and design level, for spacecraft intended for entry into the atmosphere of the earth and those of other planets. The twenty-two papers in this volume represent some of the most important recent advances in this field, contributed by highly qualified research scientists and engineers with intimate knowlege of current problems.

Published in 1982, 521 pp., 6×9, illus., $35.00 Mem., $55.00 List

TO ORDER WRITE: Publications Dept. AIAA, 370 L'Enfant Promenade, S.W., Washington, D.C. 20024-2518